Proceedings of DETC99
1999 ASME Design Engineering Technical Conferences
September 12-15, 1999, Las Vegas, Nevada, USA

DETC99/VIB-8015

SYNCHRONIZATION OF TWO COMMON-BASE-COUPLED NONLINEAR ROTATING-ECCENTRIC-DRIVEN SHAKERS

Martin Senator
Davidson Laboratory
Stevens Institute of Technology
Hoboken, New Jersey 07030

ABSTRACT

The synchronization, or lock-in, of two coupled, similarly sized rotating-eccentric-driven shakers is studied. The shakers are coupled only by being mounted on a common base, which is suspended on springs and dampers and constrained to translate along a line. This setup models a simplified conceptual version of a no-synchronizing-gearing counter-rotating-eccentric-driven telephone-cable-burying vibrating plow. An approximate quantitative theory of the synchronization of the rotors of these coupled nonlinear autonomous systems is developed in a form that is simple to understand and numerically evaluate. This analysis allows predicting, with good accuracy, whether or not the rotors will synchronize, and if so, to also predict transient and steady state properties of the locked-in motion.

INTRODUCTION

Often two or more similarly sized, coupled, nonlinear autonomous oscillating systems will synchronize, or lock in. This synchronization has two parts: each system adjusts its frequency slightly to a common frequency; and corresponding parts of each system oscillate (nearly) in phase with each other at the common frequency.

The classic example was reported by Huygens (1629-1695), who noticed that when two similar escapement-driven pendulum clocks were mounted near each other on the same wall, the pendulums synchronized, moving together in phase at a common frequency.

Two other examples that resemble each other are fireflies of Southeast Asia (Strogatz, 1994) and the main pack of runners in a long distance race. When many of these fireflies are close to each other they synchronize their flashings, going on and off together. And, the main pack of runners in a long distance race can sound as if they are striding and breathing as one.[1]

We expect that a useful model of an escapement driven clock would be fundamentally different from a useful model of a firefly or a runner. In addition, the coupling between two clocks mounted on the same wall seems fundamentally different from the coupling between neighboring fireflies or neighboring runners. Thus, while coupled nonlinear autonomous oscillating systems often synchronize, these examples suggest that there are at least two different types of systems and coupling mechanisms that can lead to synchronization. In this paper another nonlinear autonomous system using a different coupling mechanism is studied.

A model of a nonlinear autonomous oscillating system was developed during the design of rotating-eccentric-driven vibrating cable-burying plows (Senator, 1969). This model was developed to allow investigating the possibility of undesirable clock-like behavior of these plows (see Senator and Scerbo, 1973 and Scerbo and Senator, 1973). If the motor driving the shaker could not develop high enough torque, the shaker would not get up to

[1] I once could not see, but could hear, the main pack of runners as they passed. They sounded like a single giant running along the race course. I assume that the runners were striding in phase rather than out of phase, as this would minimize the length of the pack. I didn't observe the relation between the frequencies of the breathing sounds and the striding sounds, but I definitely thought that the breathing sounds had also synchronized.

design speed. Instead, it would run at an average speed just below a (low) damped natural frequency of the vibrating blade assembly on its suspension, forcing the blade assembly to vibrate at an undesirably high resonant amplitude. Analysis showed that this damped-natural-frequency-determined running speed would remain approximately constant over a large range of low developed torque values. Thus an under-torqued motor-powered rotating-eccentric-driven vibrating cable-plow would behave like an escapement-driven clock, in that over a large region of parameter space its oscillation frequency would almost be constant. Note, however, that the rotating-eccentric-shaker-driven nonlinear autonomous oscillating system ("clock") has a basically different fundamental nonlinearity than an escapement-driven Huygens' era clock.

Rotating-eccentric-driven shakers are sometimes built using two nearly identical (mirror-image) rotors mounted on a common base and constrained by gearing to rotate in-phase in opposite directions at the same speed. With this arrangement transverse shaking forces cancel and longitudinal shaking forces add. Except for (important practical) design details, the theory of a pair of geared rotating-eccentric-driven shakers is the same as the theory of a single shaker.

It has been observed that under some conditions two similar counter-rotating-eccentric-driven shakers mounted on a common base but not constrained by gearing to rotate in-phase will synchronize [2]. And, we may note that this common-base-coupling of two rotating-eccentric-driven shakers is fundamentally different from the coupling produced by mounting two Huygens' clocks near each other on the same wall. In particular, coupling dissipation plays an essential part in a recent explanation of the synchronization of two Huygens' clocks (Senator, 1998a). Yet, as we shall see, the common-base-coupling of two ungeared shakers is non-dissipative, appearing as nonlinear inertia force terms in the system differential equations.

First the model and differential equations of the common-base-coupled, eccentric-rotor-driven, nonlinear autonomous oscillating system are presented. Then coordinates and parameters that are natural for studying locked-in motions of this system are introduced and the differential equations are written in terms of these new quantities. Next a perturbation scheme is set up based on the assumptions that lock-in has occurred, that the two shakers have similar parameters, and that the system parameters have realistic values. Low order steady state and transient solutions of the transformed equations are then found and used to predict whether or not lock-in will occur, and if so, to predict steady state and transient system behavior. Finally, numerical integration is used to solve some specific examples to check the predictions.

[2] I have heard of a designer who actually designed and built a two-hydraulic-motor-driven non-geared-rotor counter-rotating-shaker under contract to a State Highway Department. I also heard that this device was used successfully to drive sign posts into the ground. I was told that an adjustable 'Y' valve was used in the oil supply line to the two fixed-displacement hydraulic motors that drove the rotors, and that this 'flexible gearing' might have been the reason the device worked.

A COMMON-BASE-COUPLED, TWO-SHAKER-DRIVEN, NONLINEAR OSCILLATING SYSTEM

Figure 1 shows a model that abstracts some features of a conceptual, common-base-coupled, motor-powered, two-rotating-eccentric-driven vibrating plow. The model consists of two shaker assemblies. Each has a translating stator and a rotor pinned to the stator. The total masses of the shakers are $m_i (i = 1,2)$, and the stators are constrained to translate in the same direction against linear springs of stiffnesses, k_i, and linear dampers with constants, c_i. The two stators are clamped to each other when the displacements are such that the forces in the springs are both zero. Let x denote the common translational displacement of the clamped stators, measured from this equilibrium position. Each rotor is a rigid body formed from balanced rotating mass (which has its mass center on the axis of rotation) and unbalanced rotating mass of magnitude, $m_{ecc\ i}$, which has its mass center at an eccentric distance, e_i, from its axis of rotation. Let θ_i denote the (crank) angles from the positive x direction to the lines from the axes of rotation through the mass centers of the eccentric masses. We choose opposite positive directions for the two crank angles to reflect the counter rotation of real (geared) shakers, although reversing this sign convention will not change the differential equations of the ungeared, common-base-coupled model. The rotors have mass moments of inertia, J_i, about their axes of rotation. The minimum possible values of J_i are $m_{ecc\ i} e_i^2$ and occur in the conceptual limit when the positive eccentric masses and the non-negative balanced masses are point masses (have zero radii of gyration about their mass centers). Rotational dampers exert frictional resisting moments between the rotors and stators of magnitudes $c_{rot\ i}\dot{\theta}_i$. Part of each balanced rotating mass and part of each translating mass form each driving motor, which exerts its developed torque between its rotor and its stator. The developed torques are modeled as decreasing linearly with speed. Thus the developed torque-speed characteristics of the driving motors are $T_{dev\ i} = T_{intercept\ i} - c_{mot\ i}\dot{\theta}_i$. The rotational friction coefficients and the negative slopes of the motor torque-speed characteristics appear in the differential equations in exactly the same way; therefore we economize on parameters and use their sums, $D_i = c_{rot\ i} + c_{mot\ i}$, as equivalent total rotational friction parameters.

The differential equations of the model are

$$[m_1+m_2]\ddot{x}+[c_1+c_2]\dot{x}+[k_1+k_2]x = (m_{ecc}e)_1\dot{\theta}_1^2\cos\theta_1+(m_{ecc}e)_1\ddot{\theta}_1\sin\theta_1 + (m_{ecc}e)_2\dot{\theta}_2^2\cos\theta_2+(m_{ecc}e)_2\ddot{\theta}_2\sin\theta_2; \quad (1)$$

$$J_1\ddot{\theta}_1 = T_{intercept\ 1} - D_1\dot{\theta}_1 + (m_{ecc}e)_1\ddot{x}\sin\theta_1; \quad (2)$$

$$J_2\ddot{\theta}_2 = T_{intercept\ 2} - D_2\dot{\theta}_2 + (m_{ecc}e)_2\ddot{x}\sin\theta_2. \quad (3)$$

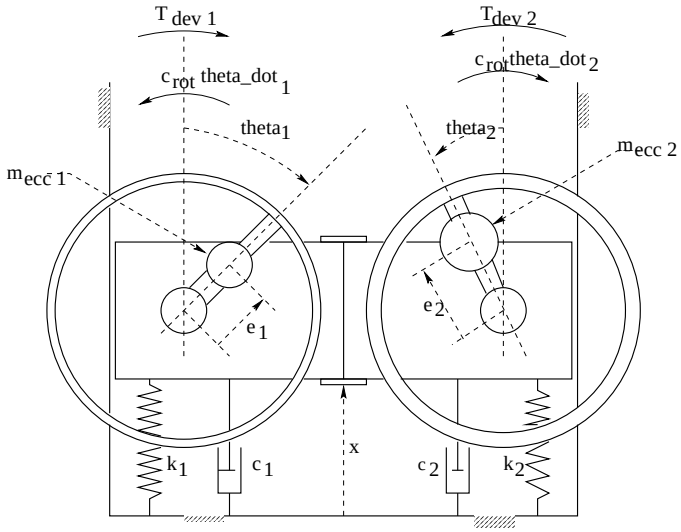

Figure 1. COMMON BASE COUPLED, TWO ECCENTRIC DRIVEN, NONLINEAR OSCILLATING SYSTEM

These equations are natural extensions of the single shaker equations. We can view the translational differential equation as stating that the sum of the individual total masses, the sum of the two spring stiffnesses, and the sum of the two damping constants form a passive translational system that is driven by the sum of rotational inertia force terms generated by the individual cranks. Similarly, we can view the rotational equations as stating that each rotor is a passive system with rotational inertia and friction that is driven by a constant applied moment and a nonlinear interaction term. The nonlinear interaction terms arise because the mass centers of the eccentric masses have acceleration components equal to the translational acceleration, $\ddot{x}$; therefore the bearings and motors must exert appropriate forces and moments to develop the required accelerating force components that act through the offset mass centers of the eccentric masses. The coupling is due to each rotor driving the common base, and to the acceleration, $\ddot{x}$, of the common base interacting with each rotor. We see that, as noted earlier, the coupling is non-dissipative, being "inertia force" generated.

FINDING LOCKED-IN SOLUTIONS

To find solutions of Eqs. (1-3) that demonstrate lock-in, start by linearly introducing two new angular variables that are natural for studying lock-in. Let θ_{av} be the average of the angular displacements of the two rotors and θ_{hd} be the half difference of the angular displacements of the two rotors,

$$\theta_{av} = (1/2)\theta_1 + (1/2)\theta_2 \text{ and } \theta_{hd} = (1/2)\theta_1 - (1/2)\theta_2. \quad (4)$$

Also, since we expect shakers that might lock in to be similar in size, introduce new average and half difference parameters that are natural for studying lock-in, as for example,

$$J_{av} = (1/2)J_1 + (1/2)J_2 \text{ and } J_{hd} = (1/2)J_1 - (1/2)J_2, \quad (5)$$

where J can be replaced by the other parameters that appear in the rotational equations, $(m_{ecc}e)$, D, and $T_{intercept}$, and by the translational parameters, m, k, and c. It turns out (as we might expect because the two clamped bases form one rigid body) that the half difference translational parameters, k_{hd}, m_{hd}, and c_{hd}, do not enter into the formulation. Since m_{ecc} and e only enter the dimensional formulation explicitly as the product, $m_{ecc}e$, we economize on parameters by assuming that each shaker has the same eccentricity, accounting for any differences (without loss of generality) by adjusting the combined parameters, $(m_{ecc}e)_{av}$ and $(m_{ecc}e)_{hd}$.

The translational equation, Eq. (1), can be expressed in terms of these average and half-difference variables and parameters as

$$\begin{aligned} m_{av}\ddot{x} + c_{av}\dot{x} + k_{av}x = (m_{ecc}e)_{av} \cdot [&(\dot{\theta}_{av}^2 + \dot{\theta}_{hd}^2)(\cos\theta_{av}\cos\theta_{hd}) \\ &- (2\dot{\theta}_{av}\dot{\theta}_{hd})(\sin\theta_{av}\sin\theta_{hd}) + (\ddot{\theta}_{av})(\sin\theta_{av}\cos\theta_{hd}) \\ &+ (\ddot{\theta}_{hd})(\cos\theta_{av}\sin\theta_{hd})] \\ + (m_{ecc}e)_{hd} \cdot [&(2\dot{\theta}_{av}\dot{\theta}_{hd})(\cos\theta_{av}\cos\theta_{hd}) \\ &- (\dot{\theta}_{av}^2 + \dot{\theta}_{hd}^2)(\sin\theta_{av}\sin\theta_{hd}) + (\ddot{\theta}_{hd})(\sin\theta_{av}\cos\theta_{hd}) \\ &+ (\ddot{\theta}_{av})(\cos\theta_{av}\sin\theta_{hd})]. \end{aligned} \quad (6)$$

Similarly, the two rotational equations, Eqs. (2,3), can be combined and expressed in terms of these average and half-difference variables and parameters as

$$\begin{aligned} J_{av}[1 - J_{hd}^2/J_{av}^2]\ddot{\theta}_{av} = &[(T_{intercept})_{av} - (J_{hd}/J_{av})(T_{intercept})_{hd}] \\ &- [D_{av} - (J_{hd}/J_{av})D_{hd}]\dot{\theta}_{av} - [D_{hd} - (J_{hd}/J_{av})D_{av}]\dot{\theta}_{hd} \\ &+ [(m_{ecc}e)_{av} - (J_{hd}/J_{av})(m_{ecc}e)_{hd}]\ddot{x}\sin\theta_{av}\cos\theta_{hd} \\ &+ [(m_{ecc}e)_{hd} - (J_{hd}/J_{av})(m_{ecc}e)_{av}]\ddot{x}\cos\theta_{av}\sin\theta_{hd} \end{aligned} \quad (7)$$

and

$$\begin{aligned} J_{av}[1 - J_{hd}^2/J_{av}^2]\ddot{\theta}_{hd} = &[(T_{intercept})_{hd} - (J_{hd}/J_{av})(T_{intercept})_{av}] \\ &- [D_{hd} - (J_{hd}/J_{av})D_{av}]\dot{\theta}_{av} - [D_{av} - (J_{hd}/J_{av})D_{hd}]\dot{\theta}_{hd} \\ &+ [(m_{ecc}e)_{hd} - (J_{hd}/J_{av})(m_{ecc}e)_{av}]\ddot{x}\sin\theta_{av}\cos\theta_{hd} \\ &+ [(m_{ecc}e)_{av} - (J_{hd}/J_{av})(m_{ecc}e)_{hd}]\ddot{x}\cos\theta_{av}\sin\theta_{hd}. \end{aligned} \quad (8)$$

For a pair of geared shakers the shakers would be made as similar as practical; that is, the magnitudes of the four rotational half difference parameters would be made negligibly small compared to their necessarily positive average values. Additionally, for a pair of geared shakers the half difference angle and its derivatives would always be negligibly small (ideally identically zero). Thus, for a pair of geared shakers the differential equation, Eq. (8), would become irrelevant, and Eqs. (6,7) would reduce to the equations of a single shaker system. This suggests that for ungeared shakers, by making the ratios of the magnitudes of all

half difference to average (rotational) parameter values small and by assuming that lock-in has occurred, we can find solutions of the common base coupled differential equations using methods generalized from those used on single shaker systems.

Start this program by introducing an expansion parameter, ε, that determines the level at which terms first appear in the expanded differential equations and expand the three dependent variables as

$$x(t) = x_0(t) + \varepsilon^1 x_1(t) + \cdots; \qquad (9a)$$

$$\theta_{av}(t) = \theta_{av\,0}(t) + \varepsilon^1 \theta_{av\,1}(t) + \cdots; \qquad (9b)$$

$$\theta_{hd}(t) = \qquad \varepsilon^1 \theta_{hd\,1}(t) + \cdots. \qquad (9c)$$

The assumption that lock-in occurs requires that the variable, θ_{hd}, is always small; this assumption is built into the solution by starting the expansion of θ_{hd} at the ε^1 level. Next, the assumption that the two shakers are similar is built into the solution by multiplying each half difference parameter in the differential equations by the bookkeeping parameter, ε. Lastly, to get a consistent solution (for a reason to be explained later), the right hand side of the average angle differential equation, Eq. (7), is also multiplied by ε.

Using these expansions, the ε^0 level θ_{av} differential equation becomes $J_{av}\ddot{\theta}_{av\,0} \equiv 0$ with solutions $\dot{\theta}_{av\,0}(t) = \omega_{av}$ and $\theta_{av\,0}(t) = \omega_{av}t + \theta_0$, where ω_{av} and θ_0 are constants that represent steady state values of average crank speed and average crank initial position. The steady state average crank speed is to be evaluated as an implicit function of the parameters as the solution proceeds. The average crank initial position depends on the arbitrary zero of time and can be taken to be zero.

Now expand the as yet unknown steady state average crank speed when it appears outside the argument of trigonometric functions as $\omega_{av} = \omega_{av\,0} + \varepsilon^1\omega_{av\,1} + \cdots$; introduce a new dimensionless independent variable, τ, by $\tau = \omega_{av}t$; and denote differentiation with respect to τ by a prime.

Using these definitions and results, the ε^0 level translational differential equation becomes

$$m_{av}\omega_{av\,0}^2 x_0'' + c_{av}\omega_{av\,0}x_0' + k_{av}x_0 = (m_{ecc}e)_{av}\omega_{av\,0}^2\cos\tau\,. \qquad (10)$$

The steady state solution of Eq. (10) is

$$x_0(t) = a_{av\,0}\cos(\omega_{av}t - \delta_{av\,0})\,; \qquad (11)$$

with the constants $a_{av\,0}$ and $\delta_{av\,0}$ given by

$$a_{av\,0} = \frac{(m_{ecc}e)_{av}\omega_{av\,0}^2}{\sqrt{[k_{av} - m_{av}\omega_{av\,0}^2]^2 + [c_{av}\omega_{av\,0}]^2}} \qquad (12)$$

and

$$\delta_{av\,0} = \arctan\left(\frac{c_{av}\omega_{av\,0}}{k_{av} - m_{av}\omega_{av\,0}^2}\right). \qquad (13)$$

The ε^1 level average crank angle differential equation now becomes

$$J_{av}\omega_{av\,0}^2\theta_{av\,1}'' = (T_{intercept})_{av} - D_{av}\omega_{av\,0} + (m_{ecc}e)_{av}\omega_{av\,0}^2 x_0''\sin\tau. \qquad (14)$$

Next, use Eqs. (11-13) to evaluate x_0'' in Eq. (14). The x_0'' term becomes the product of two same frequency out of phase trigonometric terms and so can be replaced by the sum of a zero frequency term (a constant) and a double frequency term. Continuing the solution, set the sum of all the constant terms on the right hand side of Eq. (14) equal to zero. This makes the steady state average value of $\theta_{av\,1}'(t)$ zero, so that $\theta_{av\,1}(t)$ can remain small as required by the expansion, Eq. (9b). Setting the sum of all constant terms to zero in Eq. (14) and solving for the steady state solution of what remains gives (implicit) equations for evaluating the first approximation to the unknown average crank speed, $\omega_{av\,0}$, and a steady state solution for $\theta_{av\,1}(t)$ as,

$$(T_{intercept})_{av} = D_{av}\omega_{av\,0} + (m_{ecc}e)_{av}(a_{av\,0}\omega_{av\,0}^2)(1/2)\sin\delta_{av\,0}; \qquad (15a)$$

or

$$(T_{intercept})_{av} = D_{av}\omega_{av\,0} + \frac{[(m_{ecc}e)_{av}\omega_{av\,0}^2]^2(c_{av}\omega_{av\,0})}{2[(k_{av} - m_{av}\omega_{av\,0}^2)^2 + (c_{av}\omega_{av\,0})^2]}\,; \qquad (15b)$$

and

$$\theta_{av\,1}(t) = \theta_{av\,ampl}\sin(2\omega_{av}t - \delta_{av\,0})\,; \qquad (15c)$$

with amplitude, $\theta_{av\,ampl}$, satisfying

$$\theta_{av\,ampl} = (1/8)a_{av\,0}(m_{ecc}e)_{av}/J_{av}. \qquad (15d)$$

(An integration constant in Eq. (15c) has been made zero by an appropriate (small) adjustment of the zero of time.)

The constant and double frequency forcing terms generated by the nonlinear coupling term in Eq. (14) appear at the same time. They both come from the trigonometric identity relating the product of two out-of-phase, same frequency harmonic terms to the sum of a difference frequency harmonic term and a sum frequency harmonic term. Since these two terms appear together, a consistent treatment should consider both of these terms at the same level. This, then, is the promised reason for having multiplied the right hand side of Eq. (7) by ε. If this multiplication had not been done, the sum of the constant terms would have had to be set equal to zero at the ε^0 level and the "left over" double frequency term, which also appeared at this level, would have had to be moved down to the ε^1 level and considered later.

Low Order Half Difference Rotational Displacement Equation

So far the solution for the locked-in common-base-coupled system is virtually the same as the solution for the one-shaker system. We take the decisive step when we consider the ε^1 level θ_{hd} differential equation,

$$\begin{aligned} J_{av}\omega_{av\,0}^2\theta_{hd\,1}'' + D_{av}\omega_{av\,0}\theta_{hd\,1}' - (m_{ecc}e)_{av}\omega_{av\,0}^2 x_0''(\cos\tau)\theta_{hd\,1} = \\ [(T_{intercept})_{hd} - (J_{hd}/J_{av})(T_{intercept})_{av}] \\ - [D_{hd} - (J_{hd}/J_{av})D_{av}]\omega_{av\,0} \\ + [(m_{ecc}e)_{hd} - (J_{hd}/J_{av})(m_{ecc}e)_{av}]\omega_{av\,0}^2 x_0''\sin\tau. \end{aligned} \qquad (16a)$$

Using the value of x_0'' obtained by differentiating the solution, Eqs. (11-13), transforms Eq. (16a) to

$$J_{av}\omega_{av\,0}^2\theta_{hd\,1}'' + D_{av}\omega_{av\,0}\,\theta_{hd\,1}' + K_{eq}\,\theta_{hd\,1} + K_{pf}\theta_{hd\,1}\cos(2\tau - \delta_{av\,0}) = T_{eq} - T_h\sin(2\tau - \delta_{av\,0}); \quad (16b)$$

where the new symbols are defined by

$$\begin{aligned} K_{eq} &= (m_{ecc}e)_{av}(a_{av\,0}\omega_{av\,0}^2)(1/2)\cos\delta_{av\,0}; \\ K_{pf} &= (m_{ecc}e)_{av}(a_{av\,0}\omega_{av\,0}^2)(1/2); \\ T_{eq} &= [\,(T_{intercept})_{hd} - (J_{hd}/J_{av})(T_{intercept})_{av}] \\ &\quad - [D_{hd} - (J_{hd}/J_{av})D_{av}]\omega_{av\,0} \\ &\quad - [(m_{ecc}e)_{hd} - (J_{hd}/J_{av})(m_{ecc}e)_{av}]\cdot \\ &\qquad\qquad (a_{av\,0}\omega_{av\,0}^2)(1/2)\sin\delta_{av\,0} \\ &= -(J_{hd}/J_{av})\cdot[0] \quad \text{[by Eq. (15a)]} \\ &\quad + (T_{intercept})_{hd} - D_{hd}\omega_{av\,0} \\ &\quad - (m_{ecc}e)_{hd}(a_{av\,0}\omega_{av\,0}^2)(1/2)\sin\delta_{av\,0}; \end{aligned}$$

and

$$T_h = [(m_{ecc}e)_{hd} - (J_{hd}/J_{av})(m_{ecc}e)_{av}](a_{av\,0}\omega_{av\,0}^2)(1/2). \quad (17)$$

Features of the ε^1 level $\theta_{hd\,1}$ Differential Equation

Equation (16b), the ε^1 level differential equation for the leading term, $\theta_{hd\,1}$, of the expansion of the half difference angle, contains the essential information about the possibility of lock-in of the two cranks of the common-base-coupled two-shaker system.

First and most importantly, note that the $\theta_{hd\,1}$ differential equation not only has rotational inertia and damping terms as do the original differential equations for the crank angles θ_1 and θ_2, but it also has a (possibly positive coefficient and therefore *restoring) torsional spring term*, $K_{eq}\theta_{hd\,1}$, that has no (passive, linear) counterpart in the original rotational differential equations, Eqs. (2,3). Physically the crank angles, θ_1 and θ_2, have no natural zeros. Gravity is not included in the model, and no natural stable equilibrium angle pairs exist. No torsional springs are available to move the cranks to a favored equilibrium position. All crank angle pairs are neutrally stable equilibrium angle pairs. Yet the nonlinear coupling terms in the differential equations give rise to a possibly stable (dynamically determined) equilibrium half difference angle of zero.

Next note that Eq. (16b) contains a double frequency parametric forcing term. This parametric forcing term arises together with the torsional spring term from the expansion of the product of two out-of-phase fundamental frequency terms in a nonlinear coupling term of the half difference angle differential equation. Thus the torsional spring term and the parametric forcing term physically arise together.

Eq. (16b) is a Mathieu equation with additional terms: a linear damping term; a constant applied moment term; and an applied double frequency moment term.

When solving the lowest order translational differential equation, Eq. (10), we went directly to the applied-force-driven, steady state (particular) solution. We did this because we knew that the steady state solution would physically arise. That is, positive values for all three parameters, m_{av}, k_{av}, and c_{av}, of the related initial-condition-driven homogeneous differential equation imply that for all physically realistic points in parameter space and for all initial conditions the transient solution will decay to zero. The situation is different for Eq. (16b), the lowest order differential equation for the half difference angular displacement. The stable regions of the homogeneous part of Eq. (16b) are not obvious functions of the specified parameters, and we have to explicitly consider transient solutions before going on to steady state solutions.

The torsional spring and parametric moment parameters, K_{eq} and K_{pf}, of the homogeneous part of Eq. (16b) depend only on the values of six specified *average* parameters, m_{av}, k_{av}, c_{av}, $(m_{ecc}e)_{av}$, D_{av}, and $(T_{intercept})_{av}$. The other two parameters in the homogeneous part of Eq. (16b), the average rotational inertia and the average rotational damping, J_{av} and D_{av}, are specified directly. Thus, the stable regions of parameter space for the homogeneous part of Eq. (16b) only depend on the values of the seven specified average parameters; they are independent of the values of the four specified half difference parameters. (The values of the half difference parameters affect the values of the forcing parameters and the validity of some of the assumptions used in deriving Eq. (16b), so that these half difference parameter values do affect lock-in behavior.)

Basic Lock-In Result

Before outlining the details of finding approximate stable regions and solutions of the $\theta_{hd\,1}$ differential equation, it is useful to look at a summary of the results. The basic result is that if the first approximation to the phase lag, $\delta_{av\,0}$, of the translational displacement with respect to average crank position is in the first quadrant (its cosine is positive), and if the two only-common-base-coupled shakers are similar enough (i.e., the magnitudes of all four half difference to average parameter ratios are small), then lock-in is predicted for small enough initial conditions on the half difference angular displacement and velocity and small enough departures from approximate steady-state-derived initial conditions on translational and average angular displacement and velocity. Thus lock-in is predicted to be possible only when the shakers are running in the part of the high amplitude, low frequency resonant mode in which the translational phase lag does not exceed $\pi/2$.

The basic physical requirement for this theory to be useful is that the parameters are such that average crank speed is approximately constant. When this basic requirement is satisfied and when lock-in is predicted, the transient behavior of the half difference angle is predicted to be dominated by a decaying oscillation, with frequency and rate of decay determined by the

rotational inertia, rotational damping, and torsional spring constants of Eq. (16b). The steady state of the half difference angle is predicted to be approximately the sum of a constant angle caused mostly by the constant term on the right hand side of Eq. (16b) interacting with the torsional spring, and a harmonically varying at double frequency angle, caused by both the parametric forcing term and the double frequency term on the right hand side of Eq. (16b) interacting with the rotational inertia, the rotational damping, and the torsional spring. Thus, when lock-in is predicted, we can, in a straightforward way, quantitatively characterize the general transient and steady state behavior of the locked in system.

Lock-In Results — Some Details

Detailed lock-in results are presented in (Senator, 1998b). Here an outline of procedures is sketched and the resulting equations are presented. The linearity of the low order half difference angle differential equation allows examining the transient and the two steady state forced solutions separately.

Stability of the Damped Mathieu Equation. Introduce the notation

$$\beta = \frac{K_{eq}}{J_{av}\omega_{av\,0}^2}; \gamma = \frac{K_{pf}}{J_{av}\omega_{av\,0}^2}; \eta = \frac{D_{av}}{J_{av}\omega_{av\,0}}; j_{av} = \frac{J_{av}}{(m_{ecc}e)_{av}e_{av}}; \tag{18}$$

use Eqs.(12,13,17) to find

$$\beta = \frac{a_{av\,0}}{e_{av}}\frac{\cos\delta_{av\,0}}{2j_{av}} = \frac{(m_{ecc}e)_{av}}{2j_{av}e_{av}} \cdot \frac{\omega_{av\,0}^2[k_{av} - m_{av}\omega_{av\,0}^2]}{[k_{av} - m_{av}\omega_{av\,0}^2]^2 + [c_{av}\omega_{av\,0}]^2}; \tag{19}$$

$$\gamma = \frac{a_{av\,0}}{e_{av}}\frac{1}{2j_{av}} = \frac{(m_{ecc}e)_{av}}{2j_{av}e_{av}} \cdot \frac{\omega_{av\,0}^2}{\sqrt{[k_{av} - m_{av}\omega_{av\,0}^2]^2 + [c_{av}\omega_{av\,0}]^2}}; \tag{20}$$

and write the damped Mathieu equation part of Eq. (16b) as

$$\theta''_{hd\,1} + \eta\theta'_{hd\,1} + \beta\theta_{hd\,1} + \gamma\theta_{hd\,1}\cos(2\tau - \delta_{av\,0}) = 0. \tag{21}$$

Note that in Eqs. (18-20) we are using the quantity, $\omega_{av\,0}$, which is a function of all average parameters except J_{av}, as a proxy for the average parameter, $(T_{intercept})_{av}$. Instead of specifying six average parameters and calculating $\omega_{av\,0}$ and the other average-parameter-determined quantities, we simplify the calculations by specifying five average parameters and $\omega_{av\,0}$ and then calculating $(T_{intercept})_{av}$ and the other average-parameter-determined quantities.

Low Frequency Stability. The uncancelled $\omega_{av\,0}$ in the denominator of η makes the dimensionless damping large at low average crank speeds. So at low average crank speeds it is straightforward to show that the homogeneous, damped Mathieu equation only has stable solutions when $\beta > 0$. Tracing through the definitions we see that this requires that $\delta_{av\,0} < \pi/2$.

Intermediate and High Frequency Stability. At intermediate and high average rotational speeds the dimensionless torsional damping, η, becomes small, and the stability of the damped Mathieu equation can be examined using a technique that is useful for small dimensionless parametric forcing magnitude, γ, and small damping η (see Stoker, 1950 and Nayfeh and Mook, 1979). In this technique the leading terms of expansions of $\beta_{periodic}(\gamma,\eta)$ in small powers of γ and η are found so that for the parameter sets, $(\gamma,\eta,\beta_{periodic})$, periodic solutions of the damped Mathieu equation exist. Locus curves in the (β,γ) plane of parameter sets that allow these periodic solutions alternately bound regions in parameter space in which solutions are bounded for any initial conditions (stable regions) or become unbounded for at least some initial conditions (unstable regions). The pertinent stability boundary equations are (to higher approximations than warranted by the approximations used to derive Eq. (16b)) the one tangent to the axis of ordinates at the origin,

$$\beta_{periodic\ left} = -\frac{1}{8}\gamma^2 + \frac{1}{32}\eta^2\gamma^2 + \frac{7}{2048}\gamma^4 + \cdots; \tag{22}$$

and the one starting near ($\beta = 1,\ \gamma$ small) and heading toward lower values of β,

$$\beta_{periodic\ right} = 1 - [\frac{\gamma^2}{4} - \eta^2]^{1/2} - \frac{\gamma^2}{32} + \cdots. \tag{23}$$

For the first approximation (which we are dealing with) and for practical parameter values, Eq. (22) is the axis of ordinates, and the limits specified by Eq. (23) are always satisfied. Figure 2 shows a 'resonance curve' in the (β,γ) plane for the (realistic for a vibrating plow's shaker) dimensionless average parameter values $(m_{ecc}e)_{av}/(m_{av}e_{av}) = 0.1$; $c_{av}/\sqrt{m_{av}k_{av}} = 0.2$; $D_{av}/[\sqrt{(m_{av}k_{av})}e_{av}^2] = 0.01$; $j_{av} = 2.0$; and values of $(T_{intercept})_{av}/[k_{av}e_{av}^2]$ that produce values of $\omega_{av\,0}/\sqrt{(k_{av}/m_{av})}$ in the interval $(0,2)$. The diamond ($\diamond$) on the resonance curve of Figure 2 corresponds to $\omega_{av\,0} = 0.913\cdot\sqrt{k_{av}/m_{av}}$, which is approximately the value at which β achieves its maximum. The X's correspond to equally spaced frequency points. The solid (dashed) branches correspond to parameter values that give stable (unstable) equilibrium solutions, regions of parameter space over which an $\omega_{av\,0}$ vs $(T_{intercept})_{av}$ resonance curve has positive (negative) slope (see Senator, 1969, Morrison, 1970, and Figures 5-7).

Figure 2 also shows the lock-in boundary (low β boundary of the leftmost stable region of the damped Mathieu equation) computed from Eq. (22). Thus, to within the accuracy of the first approximation, we predict lock-in can occur for the zero right hand side case of Eq. (16b) whenever $K_{eq} > 0$, which, by Eq. (17), occurs whenever $\delta_{av\,0} < \pi/2$.

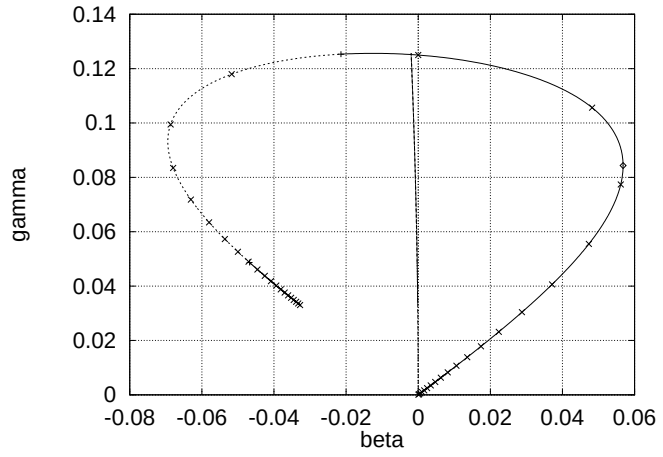

Figure 2. 'RESONANCE CURVE' IN β, γ COORDINATES AND LOW β STABILITY BOUNDARY — Parameter Values: $c_{av} = 0.2$, $(m_{ecc}e)_{av} = 0.1$, $D_{av} = 0.01$, $J_{av} = 0.2$ ($m_{av} = 1$, $k_{av} = 1$, and $e_{av} = 1$).

Quantitatively Predicting Features of Stable Transient Solutions. Simple and useful approximations to the stable transient solutions of the homogeneous part of Eq. (16b) can be found by generalizing the method used to find the stability boundaries. Expand the dependent variable in powers of a bookkeeping parameter, ε, and also multiply the parametric forcing term by ε. This allows us to first deal with the free damped (transient) vibration of a passive torsional, (J_{av} D_{av} K_{eq}) system and then to consider the (parametric) forcing of this system produced by the product of the initial transient solution, the double frequency cosine term, and the parametric forcing coefficient. Note that we can quantitatively characterize transient solutions without actually carrying out this process in detail.

Thus, from the parameters, J_{av} and D_{av}, and the average-parameter-value-determined, positive-for-a-locked-in-system, intermediate quantity, K_{eq}, define torsional average-parameter-value-determined angular frequencies by

$$\begin{aligned} \omega_{n\ tor}^2 &= K_{eq}/J_{av}; \\ \omega_{decay\ tor} &= D_{av}/(2J_{av}); \\ \omega_{nd\ tor}^2 &= \omega_{n\ tor}^2 - \omega_{decay\ tor}^2; \end{aligned} \tag{24}$$

and calculate the torsional "period," the half cycle torsional amplitude decay factor, and the five-time-constant-settling-time by

$$\begin{aligned} T_{nd} &= 2\pi/\omega_{nd\ tor}; \\ HCTADF &= \exp(-\pi\omega_{decay\ tor}/\omega_{nd\ tor}); \\ T_{settling\ tor} &= 5/\omega_{decay\ tor}. \end{aligned} \tag{25}$$

We would then approximately describe the transient solution as the superposition of two decaying oscillations. The main one would have a damped oscillating frequency of $\omega_{nd\ tor}$, corresponding to times between successive stationary angular displacement values (and between successive zero crossings) of $T_{nd}/2$. The magnitude of the ratio of two successive stationary angular displacement values would be the half cycle torsional amplitude decay factor, $HCTADF$. The second decaying oscillation would be generated by the parametric forcing term. It would be a double crank frequency, $2\omega_{av\ 0}$, decaying oscillation. The combined transient solution would effectively decay to zero by the five-time-constant-settling-time, $T_{settling\ tor}$.

Steady State Constant-Moment-Generated Solution. Given that the average parameters are such that transient solutions will decay, we can use a similar technique to find approximations to steady state solutions. First consider the steady state solution of Eq. (16b) generated by the constant forcing term, T_{eq}. The ε^0 level (first) approximation would be a constant angular displacement of

$$\theta_{hd1T_{eq}(0)}(t) \;=\; \hat{\theta};\ \text{ with }\ \hat{\theta} = T_{eq}/K_{eq}. \tag{26}$$

The ε^1 level (second) approximation (correction) would be the steady state double crank frequency oscillation of the passive (J_{av}, D_{av}, K_{eq}) system parametrically forced by the first approximation. Thus,

$$\theta_{hd1T_{eq}(1)}(t) = -\hat{\theta}K_{pf}M_2\cos(2\omega_{av\ 0}t - \delta_{av\ 0} - \phi_2); \tag{27}$$

where the (average parameter determined) quantities M_2 and ϕ_2 are

$$\begin{aligned} M_i &= 1/\sqrt{[K_{eq} - (i)^2 J_{av}\omega_{av\ 0}^2]^2 + [(i)D_{av}\omega_{av\ 0}]^2}; \\ \phi_i &= \arctan\frac{(i)D_{av}\omega_{av\ 0}}{K_{eq}\ -\ (i)^2 J_{av}\omega_{av\ 0}^2}; \qquad i = 2,4,\cdots; \end{aligned} \tag{28}$$

with $i = 2$.

We quantitatively predict then, that for a locked in system, the small constant moment, T_{eq}, will approximately produce a constant steady state half difference crank angle, $\hat{\theta}$, and a superposed double crank frequency oscillation with a (smaller) angular displacement amplitude of

$$\theta_{(1)}^* = \hat{\theta}K_{pf}M_2\ , \tag{29}$$

and an angular velocity amplitude of $2\omega_{av\ 0}\theta_{(1)}^*$.

Steady State Applied Harmonic Moment Generated Solution. We find an approximate steady state solution produced by the applied harmonic moment term, $-T_h \sin(2\omega_{av\,0}t - \delta_{av\,0})$, in a similar way. The first approximation is

$$\theta_{hd1T_h(0)}(t) = \bar{\theta}\sin(2\omega_{av\,0}t - \delta_{av\,0} - \phi_2); \text{ with } \bar{\theta} = -T_h M_2. \tag{30}$$

The second approximation is generated by the first approximation parametrically forcing the passive system. We find

$$\theta_{hd1T_h(1)}(t) = (\bar{\theta}K_{pf}\sin\phi_2)/(2K_{eq}) - (\bar{\theta}K_{pf}M_4/2)\sin(4\omega_{av\,0}t - 2\delta_{av\,0} - \phi_2 - \phi_4). \tag{31}$$

We quantitatively predict then, that for a locked in system, the small T_h-caused motion will approximately be a dominating double frequency term having angular displacement and velocity amplitudes, $\bar{\theta}$ and $2\omega_{av\,0}\bar{\theta}$, together with smaller constant and quadruple frequency terms. The value of the constant term would be

$$\theta^{**}_{(1)} = \bar{\theta}K_{pf}\sin\phi_2/(2K_{eq}). \tag{32}$$

Limits of the Approximate Theory. The foregoing theory allows us to quantitatively, but approximately, predict lock-in behavior of the common base coupled, two shaker system in a non-computationally-intensive way. Limits on the approximate theory are discussed in this subsection.

Analogous to the corresponding equilibrium and stability theory of single and geared shaker systems, the theory only produces useful results if the (average) parameter values are such that predicted average rotational speed is nearly constant. Thus, for the expansion, Eq. (9b), to lead to useful numerical results, the maximum of $|\dot{\theta}_{av\,1}(t)|$ over a crank revolution should be small compared to the corresponding maximum of $|\dot{\theta}_{av\,0}(t)|(= \omega_{av\,0})$. From the solution for $\theta_{av\,0}$ and Eqs. (12, 15c,d, 18) this requirement becomes

$$R = \frac{1}{4j_{av}}\frac{a_{av\,0}}{e_{av}} \ll 1. \tag{33}$$

For fixed values of the reference average parameters, k_{av}, m_{av}, and e_{av}; of the dimensionless average translational damping, $c_{av}/\sqrt{(k_{av}m_{av})}$; and of the dimensionless average rotational inertia multiplier, j_{av}; and for the proxy average parameter, $\omega_{av\,0} = 1 \cdot \sqrt{(k_{av}/m_{av})}$, a value at which $a_{av\,0}$ approximately achieves its maximum value, the dimensionless quantity, R, also approximately achieves its maximum value of

$$R_{max} \approx \frac{1}{4j_{av}}\frac{(m_{ecc}e)_{av}}{m_{av}e_{av}}\frac{1}{c_{av}/\sqrt{(k_{av}m_{av})}}. \tag{34}$$

As an example, R_{max} for the representative systems of Figure 2 is approximately 1/16; therefore the theory can be useful for these systems.

The additional basic physical assumption for common base coupled shakers, that lock-in occurs, has two related parts. Firstly, and directly, the half difference angle must always be small, of order ε^1. This allows replacing the sine and cosine of the small half difference angle by the half difference angle and by one, and gives part of the transition from Eq. (8) to the ε^1 level equation, Eq. (16a). Secondly, for the terms in Eq. (8) that generate the right hand side of Eq. (16a) to be at the ε^1 level, the ratios of the magnitudes of all four half difference parameters to their average values, r_T, r_D, r_M, and r_J, must be small, of order ε^1.

NUMERICAL CHECKS

In this section the theoretical results are checked by numerically integrating some specific examples of the differential equations. Five systems were studied numerically, each using average parameter values that correspond to the diamond ($\diamond$) in Figure 2 and each using a different set of the four half difference parameter ratios. Since these average parameter values determine a phase lag, $\delta_{av\,0}$, of the first approximation to translational displacement with respect to average rotational displacement that is less than $\pi/2$, lock-in is predicted to occur whenever all four half difference parameter ratios and the calculated steady state average value of half difference angular displacement are small enough for the theory to apply. The first three examples satisfy these conditions. The fourth example considers a case with the half difference parameters no longer small; they are large enough so that the constant part of the predicted steady state half difference angle, computed as if the theory still applies for large half difference parameter ratios, exceeds one quarter revolution. Since such a large half difference angle corresponds to the two eccentrics locking up while pulling against each other, we guess that lock-in is unlikely to occur for this case. (We cannot be more certain without considering terms that were neglected in order to develop the simplified approximate theory.) In the fifth example a hypothesis, suggested by the numerical results of the other examples, for predicting intermediate magnitude transition (bifurcation) values of half difference parameters at which lock-in behavior stops is investigated and shown to work for this example.

Proportional Shakers, T_{eq}-Only Shakers, and T_h-Only Shakers

All five examples share the average-parameter-determined quantities shown in Table 1. The magnitudes of all four half difference parameter ratios for the first three examples were chosen to be $1/20$, an acceptably small quantity (just slightly larger than the value of R). With these small ratios we are confident that the

Table 1. AVERAGE PARAMETER DETERMINED QUANTITIES FOR THE EXAMPLES.

Symbol	Value	Symbol	Value
c_{av}	0.2	D_{av}	0.01
$(m_{ecc}e)_{av}$	0.1	J_{av}	0.2
$\omega_{av\ 0}$	0.9130	$(T_{intercept})_{av}$	0.01952
$a_{av\ 0}$	0.3374	$\delta_{av\ 0}$	47.65°
R	0.04217	T_{nd}	29.06
$HCTADF$	0.6954	$T_{settling\ tor}$	200.0
M_2	1.521	ϕ_2	178.4°
M_4	0.3762	ϕ_4	179.2°
K_{eq}	0.009472	K_{pf}	0.01406
$\theta_{av\ ampl}$	0.02109	$2\omega_{av\ 0}\theta_{av\ ampl}$	0.03850

average-parameter-value-controlled predictions of the approximate theory will be accurate, as will the predictions that also depend on the half difference parameter values.

For the first example positive signs were chosen for all four ratios. Having all four ratios equal (and small) creates a coupled system with zero steady state forcing; both the constant, T_{eq}, and the second harmonic, T_h, forcing terms on the right hand side of Eq. (16b) are zero. A pair of proportional shakers results, with shakers 1 and 2 having their four rotational equation parameters 21/20 and 19/20 times the corresponding average parameters.

The second example represents a T_{eq}-only pair of shakers. The intercept torque of shaker 1 is 21/20 times larger than the average intercept torque, while its total rotational damping, eccentric mass fraction, and rotational inertia are 19/20 times the average values. For shaker 2 these multipliers are interchanged.

The third example represents a T_h-only pair of shakers. The intercept torque, the total rotational damping, and the eccentric mass fraction of shaker 1 are each 21/20 times larger than the corresponding average values, while the rotational inertia of shaker 1 is 19/20 times the average value. For shaker 2 these multipliers are interchanged.

Since these three examples have identical average parameter values, the predicted steady state translational and average angular displacements and velocities are identical. Table 2 compares some predicted and accurately calculated characterizing values for the translational and average angular motions for these examples. We see that the theory accurately predicts these characterizing values, with the greatest relative error less than 0.5% (for the maximum value of steady state average angular velocity for the T_{eq}-only example). Figure 3 compares plots of predicted and calculated values of steady state average angular velocity vs. steady state translational displacement in the T_{eq}-only example. We can see that the theory also accurately predicts translational displacement over a cycle while it (everywhere) slightly underestimates average angular velocity (with a maximum relative error less than 0.5%; see Table 2).

The proportional shaker example displays the transient behavior of θ_{hd} most clearly, since for this example the predicted steady state values of θ_{hd} and $\dot{\theta}_{hd}$ are zero. Figure 4 shows half difference angular velocity vs. time calculated over a time interval of length, $T_{settling\ tor}$.We see that the shakers do lock in as predicted and that the transient behavior of the half difference angle is accurately characterized by the four predicting quantities, T_{nd}, $HCTADF$, $T_{settling\ tor}$, and $2\omega_{av\ 0}$, of the theory. As examples of this accurate characterization note how there are just fewer than seven slow oscillations in 200.0 s compared to the predicted $200.0/29.06 = 6.882$; how the ratio of the magnitudes of any two consecutive (smoothed, low frequency) stationary half difference angular velocity values in Figure 4 are just about equal to the reciprocal of the half cycle torsional amplitude decay factor; how the transient has virtually decayed to zero at the five cycle decay time; and how there are four plus high frequency cycles of oscillation in the second positive going half T_{nd} cycle compared to the predicted value of $\omega_{av\ 0}/\omega_{nd\ tor} \approx 4.2$.

A Non-Locked-In Shaker

The half difference parameters for the fourth numerical example are chosen to almost certainly give a shaker pair that will not lock in. Note that the T_{eq}-only shaker pair (example two) had, for the small half difference parameter ratios of $r_T = +1/20$, $r_M = -1/20$, $r_D = -1/20$, and $r_J = -1/20$, a value of $T_{eq}/T_{av} = 0.1$ that produced a predicted average steady state half difference angle of 0.2061 rad. Since the approximation is linear, increasing these ratios by a factor of eight would increase the predicted steady state half difference angle by the same factor, causing the predicted steady state difference in crank angles to exceed half a revolution. And, as noted, it is hard to imagine a locked-in situation with the eccentrics pulling against each other. (The assumption that the half difference angle remains small is violated for these half difference parameter choices, but it is still likely that these choices will produce a non-locked-in example.)

Figure 5, which shows the individual crank angular velocities vs. time for this example, verifies that lock-in does not occur. (Temporarily disregard the three $\dot{\theta}_{0\ i}$ vs. $(T_{intercept})_i$ resonance curves superposed on Figure 5.) Shaker 1, which has an intercept torque 28/12 times that of shaker 2 and total rotating friction, eccentric mass fraction, and rotational inertia 12/28 times as much rotates, as expected, at a higher average steady state speed than shaker 2. For the parameter values of this example the common base coupling of the shakers produces relatively small effects. Thus at the scales of Figure 5 we can see that the steady state

Table 2. COMPARING PREDICTED AVERAGE-PARAMETER-DETERMINED CHARACTERIZING VALUES WITH ACCURATELY CALCULATED ONES.

Name	Symbol	Predicted Values	Calculated Steady State Values (for 200s of integration.)		
		All Shakers	Proportional Shakers	T_{eq} only Shakers	T_h only Shakers
Disp. Ampl.	$a_{av\ 0}$	0.3374	0.3372	0.3361	0.3372
Vel. Ampl.	$a_{av\ 0}\omega_{av\ 0}$	0.3080	0.3073	0.3073	0.3073
$\max(\dot{\theta}_{av})$	$\omega_{av\ 0}\cdot$ $(1+2\theta_{av\ ampl})$	0.9515	0.9541	0.9562	0.9544
midrange$(\dot{\theta}_{av})$	$\omega_{av\ 0}$	0.9130	0.9138	0.9169	0.9138
$\min(\dot{\theta}_{av})$	$\omega_{av\ 0}\cdot$ $(1-2\theta_{av\ ampl})$	0.8745	0.8734	0.8776	0.8732

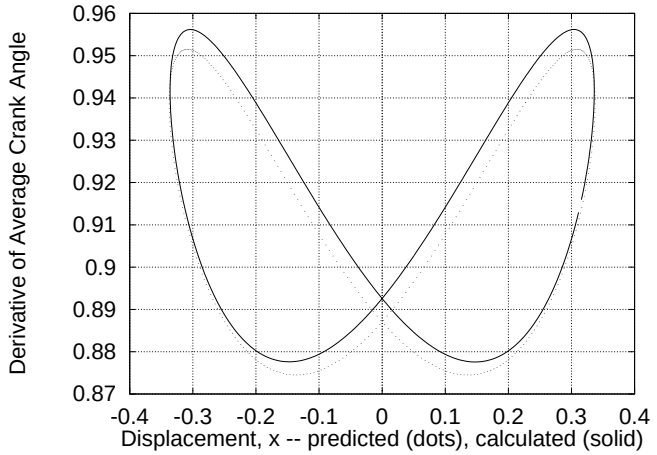

Figure 3. TIME DERIVATIVE OF AVERAGE CRANK ANGLE VS. TRANSLATIONAL DISPLACEMENT IN THE STEADY STATE FOR THE T_{eq}-ONLY EXAMPLE — Parameter Values: $c_{av} = 0.2$, $(m_{ecc}e)_{av} = 0.1$, $D_{av} = 0.01$, $J_{av} = 0.2$, $(T_{intercept})_{av} = 0.01952$, $r_M = -1/20$, $r_D = -1/20$, $r_J = -1/20$, $r_T = +1/20$.

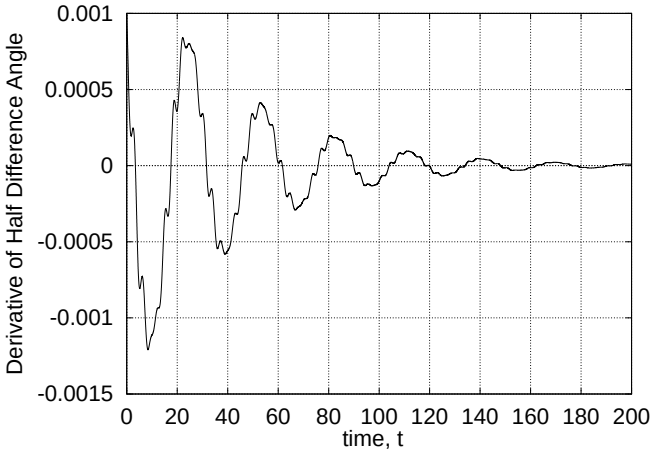

Figure 4. TIME DERIVATIVE OF HALF DIFFERENCE CRANK ANGLE VS. TIME FOR THE PROPORTIONAL SHAKERS EXAMPLE — Parameter Values: $c_{av} = 0.2$, $(m_{ecc}e)_{av} = 0.1$, $D_{av} = 0.01$, $J_{av} = 0.2$, $(T_{intercept})_{av} = 0.01952$, $r_M = +1/20$, $r_D = +1/20$, $r_J = +1/20$, $r_T = +1/20$.

angular velocity of shaker 1 has a high average value of about 4.4 rad/s; a superposed, self generated, small magnitude, double frequency component at about 8.8 rad/s; and a lower frequency component at an indeterminable frequency. Shaker 2 has a low average angular velocity of about 0.7 rad/s; a coupling component at about the average angular velocity of shaker 1; and a component at a low frequency that cannot be determined by inspection.

A Backward Prediction. Using 20-20 hindsight (or more positively, having sharpened intuition by working the four numerical examples) we can quantitatively predict the observed behaviors. Towards this end consider the three ε^1 level $\dot{\theta}_{av\ i\ 0}$ vs. $(T_{intercept})_i$ resonance curves superposed on Figure 5. The first (solid line) is a bases-clamped-together, rotors-geared-to-each-other, both-motors-on resonance curve ($i = av$); the second (medium dash line) is a bases-clamped-together, shaker 1-on, shaker 2-braked resonance curve ($i = 1$); and the third (small dash line) is a bases-clamped-together, shaker 2-on, shaker 1-

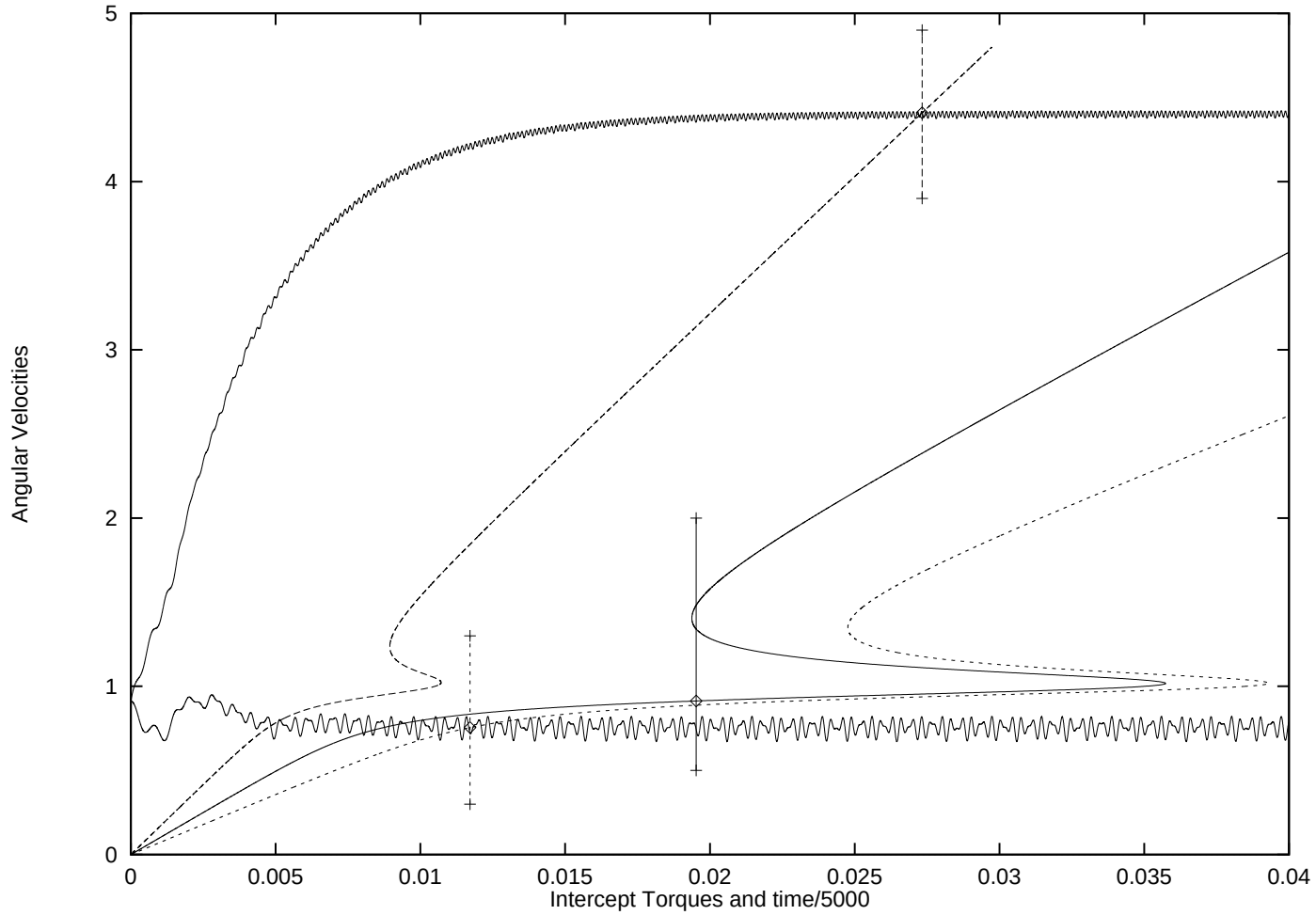

Figure 5. INDIVIDUAL CRANK SPEEDS VS. TIME AND THREE RESONANCE CURVES — SHAKERS DO NOT LOCK IN — Parameter Values: $c_{av} = 0.2$, $(m_{ecc}e)_{av} = 0.1$, $D_{av} = 0.01$, $J_{av} = 0.2$, $(T_{intercept})_{av} = 0.01952$, $r_M = 8\cdot(-1/20)$, $r_D = 8\cdot(-1/20)$, $r_J = 8\cdot(-1/20)$, $r_T = 8\cdot(+1/20)$.

braked resonance curve ($i = 2$). These curves are calculated using Eq. (15b) for the $i = av$ case and the equations formed from Eq. (15b) by substituting $D_{1\ or\ 2}$ and $(m_{ecc}e)_{1\ or\ 2}$ for D_{av} and $(m_{ecc}e)_{av}$, and $2c_{av}$, $2m_{av}$, and $2k_{av}$ for c_{av}, m_{av}, and k_{av}. First approximations to the average speed (or speeds) at which these three two-shaker combinations could run would be the ordinate (or ordinates) at which the vertical lines at $(T_{intercept})_i$ intercept the respective resonance curves.

We see that for the two one-rotor-braked cases these intersections are well beyond the knees of the resonance curves. Thus, while the both-rotors-on (geared) case has three intersections (two stable and one unstable), the shaker 1-on shaker 2-braked case has one (stable, high-frequency-branch) intersection, and the shaker 2-on shaker 1-braked case has one (stable, low-frequency-branch) intersection. We also see from the $\dot{\theta}_{1\ and\ 2}$ vs. time curves that these one-braked-shaker intersections accurately predict the average angular speeds of the two (weakly coupled) shakers.

A Half Difference Parameter Transition Prediction That May Work. We can then hypothesize as follows. Keep the translational parameters, the total rotational dampings, and the eccentric mass fractions constant. This fixes the two one-shaker-on one-shaker-braked resonance curves. Then estimate values of r_T, the ratio of half difference intercept torque to average intercept torque, that just bring both intercepts "significantly" beyond the knees (the local maximum of one and the local minimum of the other) of their curves. (A margin is necessary to allow for the resonance curves only being first approx-

imations.) Then test, by integrating the differential equations at these r_T values, whether the locked-in trajectory bifurcates at a point in parameter space at which both intercepts are beyond, but close to, the knees of the actual resonance curves. If this bifurcation is observed then the hypothesis is not disproved. Further numerical testing or analysis would be required. If, however, the bifurcation between locked-in behavior and lightly coupled behavior occurs well beyond the knees of the resonance curves, then the hypothesis has failed.

Figures 6 and 7 show, for the fifth example, resonance curves and plots of crank angles vs. time analogous to those of Figure 5. For this example the two half difference parameter ratios that affect the resonance curves, r_D and r_M, are both kept equal to -1/20, the same values as for the locked-in T_{eq}-only example. Even though the value of r_J does not affect the (ε^1 level) resonance curves, it still affects the behavior of the system. A value of -1/20, the same as for the T_{eq}-only example was chosen for this parameter. Then the differential equations were integrated for values of the intercept torque ratio, r_T, that put both intersections beyond the knees of their resonance curves. Figure 6 shows the results for $r_T = 0.13$ and Figure 7 shows the results for a neighboring value, $r_T = 0.14$. We see that at the lower value of r_T the two shakers lock in and that at the neighboring higher value the two shakers run almost independently in a lightly coupled mode. A bifurcation has occurred between these two parameter values. Studying Figures 6 and 7 we see that the hypothesis that the intersections moving slightly beyond the knees of the ε^1 level resonance curves triggers the bifurcation cannot be rejected.

SUMMARY AND CONCLUSIONS

The lock-in of two rotating-eccentric-driven common-base-coupled nonlinear oscillating shakers is studied. An approximate quantitative theory is developed that predicts whether or not two such shakers that are similar in size will lock in. Lock-in is predicted to occur when the first approximation to the phase lag, $\delta_{av\,0}$, of the translational displacement with respect to average crank angle is less than $\pi/2$. When lock-in is predicted the theory allows accurately characterizing both the transient and steady state motions of the locked-in shakers using quantities that can be calculated from the system parameters in a straightforward, non-computationally intensive way.

The theory was checked by numerically integrating the coupled system's differential equations for three cases of similarly sized shakers where lock-in is predicted. It was found that the theory accurately predicted the computationally intensive calculated results.

The theory was extended to allow guessing when lock-in will almost surely not occur because the shakers differ too much from each other in size, even though the average parameter determined phase lag, $\delta_{av\,0}$, is less than $\pi/2$. The basic idea of this extension is that if the non-applicable (because of non-small half difference parameters and non-small predicted half difference angles) theory predicts lock-in but also predicts that the two steady state crank angles are about a half revolution apart, lock-in is extremely unlikely to occur. This extension was numerically checked in one case and, as expected, lock-in did not occur.

This numerical example suggested a way of predicting individual shaker average crank speeds when parameters are such that a pair of these common-base-coupled shakers might run in a lightly coupled, non-locked-in mode. First approximations to the average crank speed vs. intercept torque characteristics of the single shaker driven systems formed by coupling the bases but only powering the motor driving one of the shakers were calculated. (For simplicity the rotor of other shaker was assumed to be braked.) For the fourth example, where the intersections of these characteristics with their actual intercept torque lines were well beyond the knees of the resonance curves (with one intersection necessarily on the high frequency branch of its characteristic and the other intersection necessarily on the low frequency branch of its characteristic), the integrations showed that these intersections accurately predicted both the high and the low average crank speeds. Physically, these non-similar shakers were weakly coupled by the common base coupling and each ran almost as if the other were turned off.

This successful (backward) prediction suggested a way of guessing sets of intermediate magnitude half difference parameter values at which a bifurcation from a locked-in motion to a lightly coupled motion might occur. (The model is based on the half difference parameters being sufficiently small, and cannot tell us how small this is.) We calculate the first approximations to the two one-shaker-on, other-shaker-braked average angular velocity vs. intercept torque resonance curves and guess that a bifurcation occurs when both intersections of these curves with the individual motor intercept torque lines move just beyond the knees of the resonance curves. This hypothesis was tested in the fifth numerical example and found to work for that particular case.

Playing around numerically with different sets of parameter values indicates that these two-coupled-shaker systems can run in different and interesting modes other than the locked-in mode analyzed here and the lightly coupled mode shown in Figures 5-7. Thus, these systems provide fruitful possibilities for further investigations.

REFERENCES

Eaton, J. W., "Octave - A high level language for interactive computations." Octave is free software. Its web page is at <http://www.che.wisc.edu/octave>.

Morrison, J. A., "Asymptotic Analysis of a Nonlinear Autonomous Vibratory System", *Bell System Technical Journal*, January, 1970, 73-80.

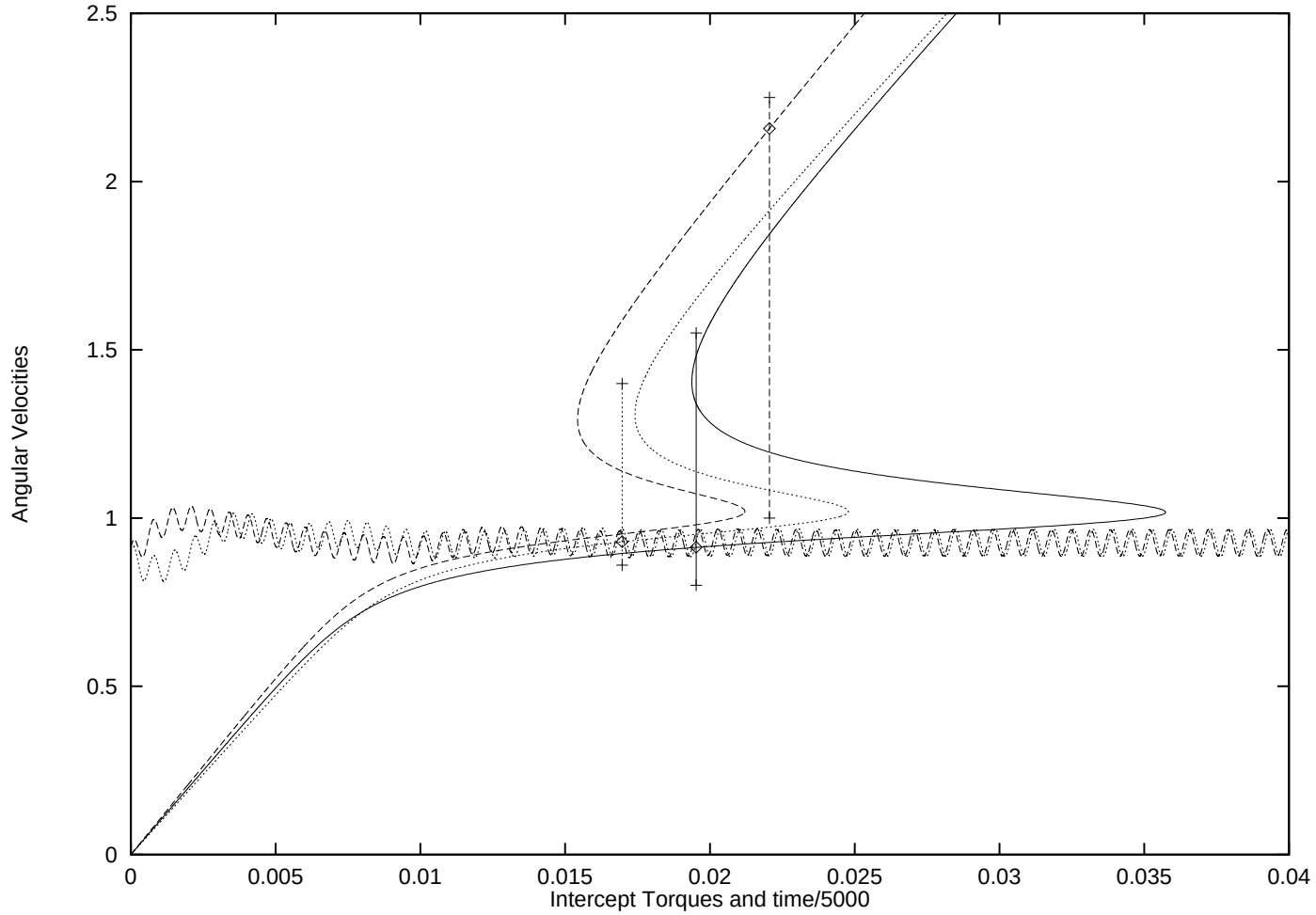

Figure 6. INDIVIDUAL CRANK SPEEDS VS. TIME AND THREE RESONANCE CURVES —SHAKERS LOCK IN — Parameter Values: $c_{av} = 0.2$, $(m_{ecc}e)_{av} = 0.1$, $D_{av} = 0.01$, $J_{av} = 0.2$, $(T_{intercept})_{av} = 0.01952$, $r_M = -1/20$, $r_D = -1/20$, $r_J = -1/20$, $r_T = +0.13$.

Nayfeh, A. H. and Mook, D. T., *Nonlinear Oscillations*, Wiley, NY, 1979, 258-301.

Scerbo, L. J., and Senator, M., "Transient Motions of Orbital Cable Plows," *The Shock and Vibration Bulletin*, Naval Research Laboratory, Washington, DC, June, 1973, 83-94.

Senator, M., "Limit Cycles and Stability of a Nonlinear Two-Degree-of-Freedom Autonomous Vibratory System," *Journal of Engineering for Industry*, Transactions of the ASME, **91**, Series B No. 4, 1969, 959-966.

Senator, M., "Synchronization of Two Coupled Escapement-Driven Huygens' Clocks," Davidson Laboratory Technical Note 1013, Stevens Institute of Technology, May, 1998.

Senator, M., "Synchronization of Two Common-Base-Coupled Nonlinear Rotating-Eccentric-Driven Shakers," Davidson Laboratory Technical Note 1014, Stevens Institute of Technology, October, 1998.

Senator, M. and Scerbo, L. J., "Steady-State Motions of Orbital Cable Plows," *The Shock and Vibration Bulletin*, Naval Research Laboratory, Washington, DC, June, 1973, 67-82.

Stoker, J. J., *Non-Linear Oscillations in Mechanical and Electrical Systems*, Interscience, NY, 1950, 202-222.

Strogatz, S. H., *Nonlinear Dynamics and Chaos*, Addison-Wesley, Reading, MA, 1994, 103-106.

ACKNOWLEDGMENT

Thanks to J. W. Eaton for developing and maintaining the (free) Octave software package used for the numerical calculations and to Miriam Senator for editorial assistance.

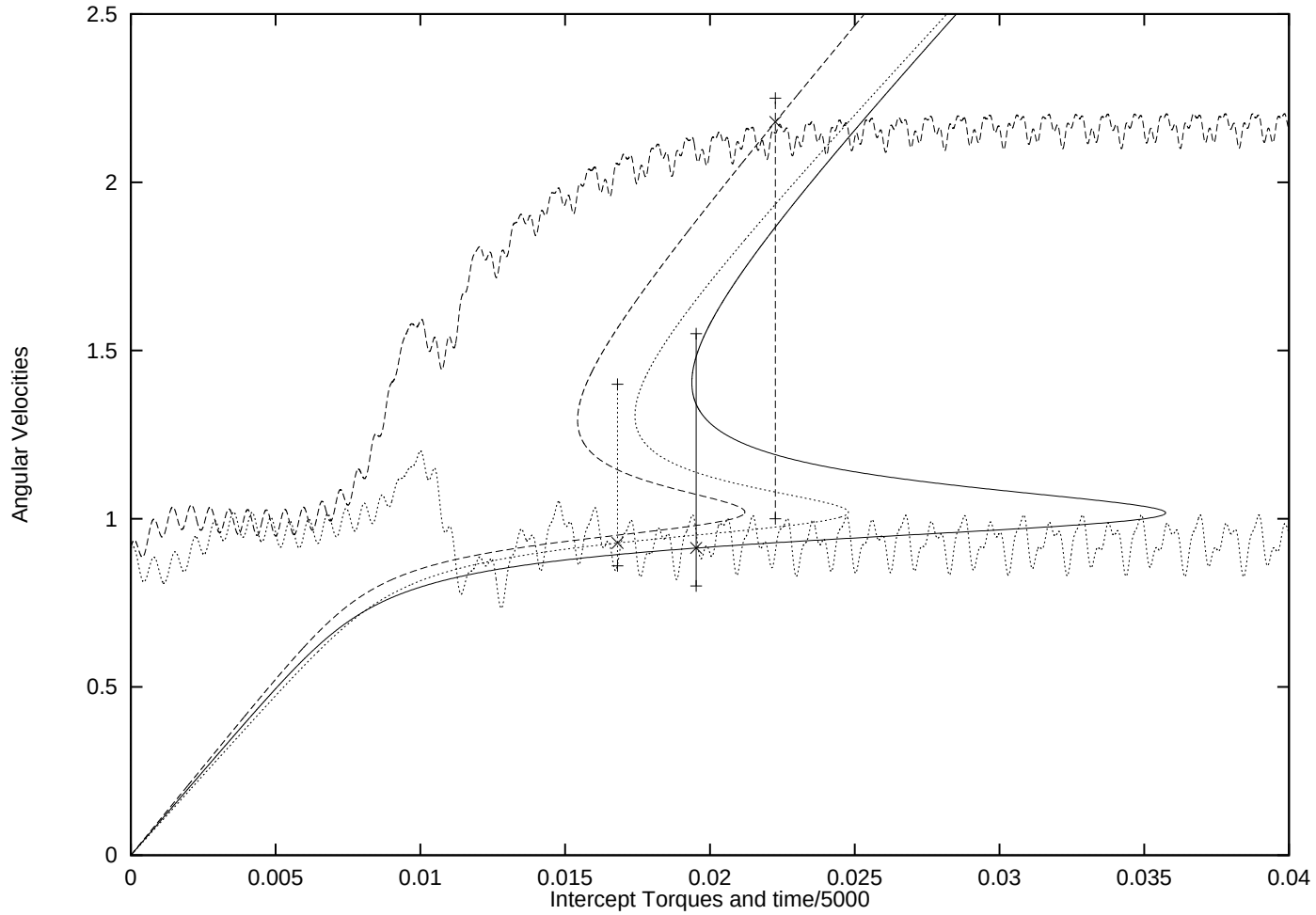

Figure 7. INDIVIDUAL CRANK SPEEDS VS. TIME AND THREE RESONANCE CURVES — SHAKERS DO NOT LOCK IN — Parameter Values: $c_{av} = 0.2$, $(m_{ecc}e)_{av} = 0.1$, $D_{av} = 0.01$, $J_{av} = 0.2$, $(T_{intercept})_{av} = 0.01952$, $r_M = -1/20$, $r_D = -1/20$, $r_J = -1/20$, $r_T = +0.14$.